Int J Adv Manuf Technol (2015) 76:1319–1332
DOI 10.1007/s00170-014-6283-8

ORIGINAL ARTICLE

Effect of milling parameters on mechanical alloying of aluminum powders

A. R. Othman · Ali Sardarinejad · Abdul Kadir Masrom

Received: 8 March 2012 / Accepted: 14 August 2014 / Published online: 17 September 2014

Abstract The solid-state interfacial state of aluminum powders was investigated upon inert gas, ball number and size, milling time, speed, and processing control agent (PCA) under high energy planetary mechanical alloying in sub-micron scale. The study observed significant variations in morphology of the milled powders at different milling parameters due to the fracturing and cold welding mechanisms. The uses of different ball numbers and sizes, and with higher rotating speed have resulted in further agglomeration. However, the adding of methanol as the PCA has provided the effective fracture mechanisms, by modifying the surface properties of the deforming particles to overcome the cold welding, hence reducing the particle sizes and changing the morphological shape to granular structures. The milling parameters have been proposed to also include 100 stainless steel balls with 10 mm in diameter, 200 rpm rotational speed, performed under the argon gas for 30 h to effectively produce finer particles and homogeneity in the particle distribution for future sintering process.

Keywords Mechanical alloying · Milling parameters · Aluminum powder · Powder characterization

A. R. Othman (✉) · A. Sardarinejad
School of Mechanical Engineering, Engineering Campus, Universiti Sains Malaysia, Nibong Tebal, Penang 14300, Malaysia
e-mail: merahim@usm.my

A. R. Othman
e-mail: abdul.r.othman@gmail.com

A. R. Othman
Advanced Composite Processing Lab, School of Aerospace Engineering, Universiti Sains Malaysia, 14300 Nibong Tebal, Pulau Pinang, Malaysia

A. K. Masrom
Advanced Materials Research Centre (AMREC) SIRIM Berhad, Kulim Hi-Tech Park, 09000 Kulim, Kedah, Malaysia

1 Introduction

1.1 Mechanical alloying

The objectives of milling process are to reduce the particle sizes (breaking down the material) mixing, blending, and particle shaping. The application of milling (ball milling) for fabrication of engineering materials via mechanical alloying (MA) process has been established over the years. Benjamin [1] has defined the MA process as a method for producing composite metal powders with a controlled fine microstructure. It occurs by repeated fracturing and re-welding of a mixture of powder particles in a highly energetic ball mill. As originally carried out, the process requires at least one fairly ductile metal (e.g., aluminum) to act as a host or binder. The major processes involve in MA for producing quality powders of alloys and compounds with well-controlled microstructure and morphology include repeated welding, fracture, and re-welding of the reactant mixed powders.

It is critical to establish a balance between fracturing and cold welding in order to obtain a successful mechanical alloying process. Two techniques were proposed to reduce cold welding and promote fracturing [2]. The first technique is to modify the surface properties of the deforming particles by adding a suitable processing control agent (PCA), which is also known as wet milling, that impedes the clean metal contact necessary for cold welding. The second technique is to modify the deformation mode of the powder particles so that they are able to deform to the large compressive strains necessary for flattening and cold welding. In addition, cooling the mill chamber was identified as an approach to accelerate the fracture and establishment of steady-state processing due to the effect of milling temperature [2]. It should be emphasized that milling the powders of certain metal which will be cold welded easily with an organic agent

(PCA) may lead to an undesired reaction between the PCA and the milled powders [3].

It was found that the powder particles are repeatedly cold welded by the multiple actions of colliding balls [4]. Whenever two grinding balls collide, a small amount of powder is trapped in between them. Typically, around 1,000 particles with an aggregate weight of about 0.2 mg are trapped during each collision. During this process, the powder morphology could be modified. For the soft powders like aluminum, the flattened layers overlap and form cold welds. This leads to formation of characteristically layered composite microstructure of powder particles consisting of various combinations of the starting ingredients [5]. The work-hardened elements or composite powder particles may fracture at the same time. These competing events of cold welding (with plastic deformation and agglomeration) and fracturing (i.e., size reduction) continue repeatedly throughout the milling period. Eventually, a refined and homogenized microstructure is obtained, and the composition of the powder particles is the same as the proportion of the starting constituent powders. Along with the cold welding event described above, some powders may also coat the grinding medium and/or the inner surface walls of the container. A thin layer of the coating is beneficial in preventing wear-and-tear of the grinding medium and also in preventing contamination of the milled powder with the debris.

1.2 Planetary ball milling

In the planetary ball mill, the milling media contains considerably high energy, as the milling stock and balls come off the inner wall of the vial (milling bowl) and the effective centrifugal force can reach up to 20 times of gravitational acceleration. The centrifugal forces caused by the rotation of the supporting disk and autonomous turning of the vial act on the milling charge (balls and powders). Since the turning directions of the supporting disk and the vial are opposite, the centrifugal forces alternately are synchronized and in opposite direction. Therefore, the milling media and the charged powders alternatively roll on the inner wall of the vial, and are subsequently lifted and thrown off across the bowl at high speed. One advantage of this type of mill is the ease of handling the vials (45 to 500 mL in volume) inside the glove box.

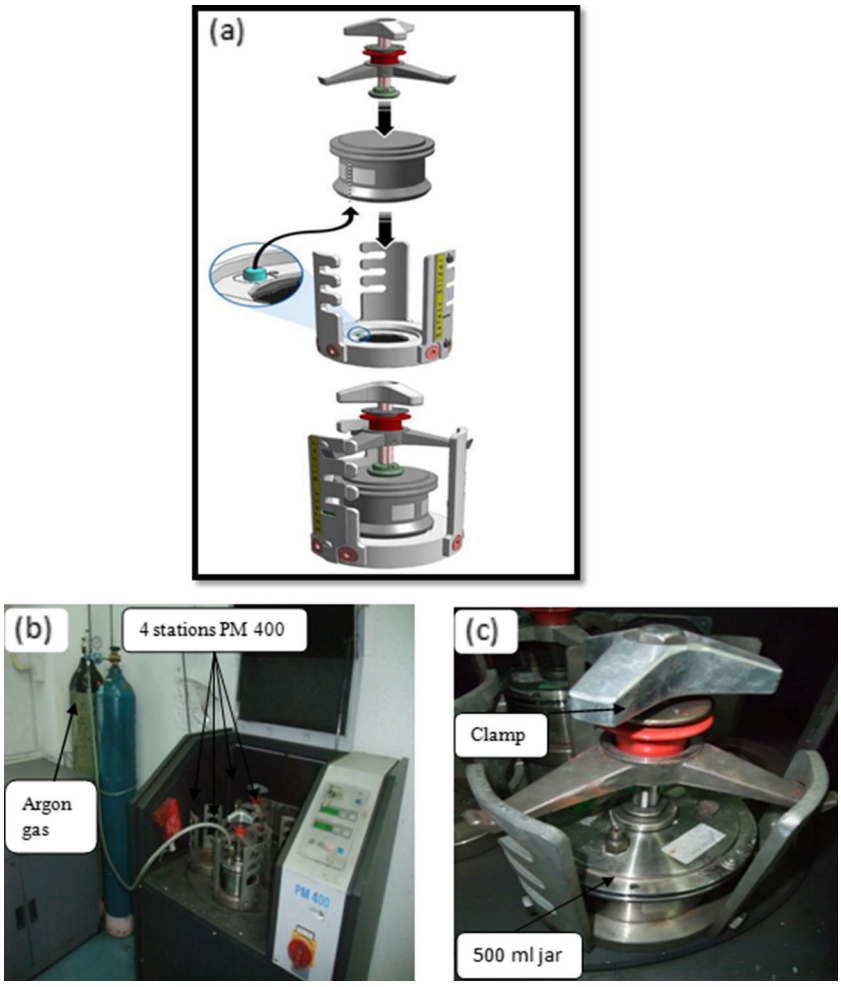

Fig. 1 **a** Clamping of milling jar; **b** Retsch PM400; **c** 500 mL jar single station

The field of nano-composites has recently attracted considerable attention as researchers strive to enhance composite properties and extend their utility by using nanoscale reinforcements instead of more conventional particulate-filled composites [6]. While smaller reinforcements have a better reinforcing effect than larger ones, applying the ball milling technique for composite fabrications provides the following merits:

- Since ball milling is processed at room temperature, the disadvantages of the liquid metallurgy method for producing undesirable materials can be avoided.
- Moreover, the ball milling process can produce homogeneous nano-composite powders in comparison to the conventional coarse particulate-filled composites.

Consolidation of milled powders is an important step for reliable and reproducible determination of the physical/mechanical properties of the fabricated materials and is required for most industrial applications [7]. However, the compaction process of the ball-milled powders into bulk, full density compaction while retaining nanoscale grain size is a major challenge [8]. Many sintering techniques, e.g., hot pressing [9] and hot extrusion [10], sintering forging [11], and HIP-ing [12], have been employed to consolidate the mechanically alloyed powder.

The MA process is significantly affected by several factors that play very important roles in the fabrication of homogeneous materials. It is well known that the quality characteristics of the milled powders of the final product, such as the particle size distribution, morphology, and the degree of disorder, depend on the milling conditions and, as such, the more complete control and monitoring of the milling conditions, the better end product is obtained. Thus, the aim of this paper is to determine the effect of different ball milling parameters and operating conditions (milling time, ball size, PCA, and speed) in aluminum matrix in order to optimize the process in achieving the particle size reduction with less contamination.

2 Experimental materials and methods

Current powder metallurgy techniques have been employed with some success in producing metal matrix composites (MMCs), which typically consist of (i) mixing and blending, (ii) consolidation, and (iii) secondary processing. Until recently, the challenges that remain were many, including particle agglomeration, inhomogeneous dispersion of particulates, as well as weak interface between particulates and matrix. In mechanical milling, work materials are placed together with some milling balls in a vial and are then moved upon the

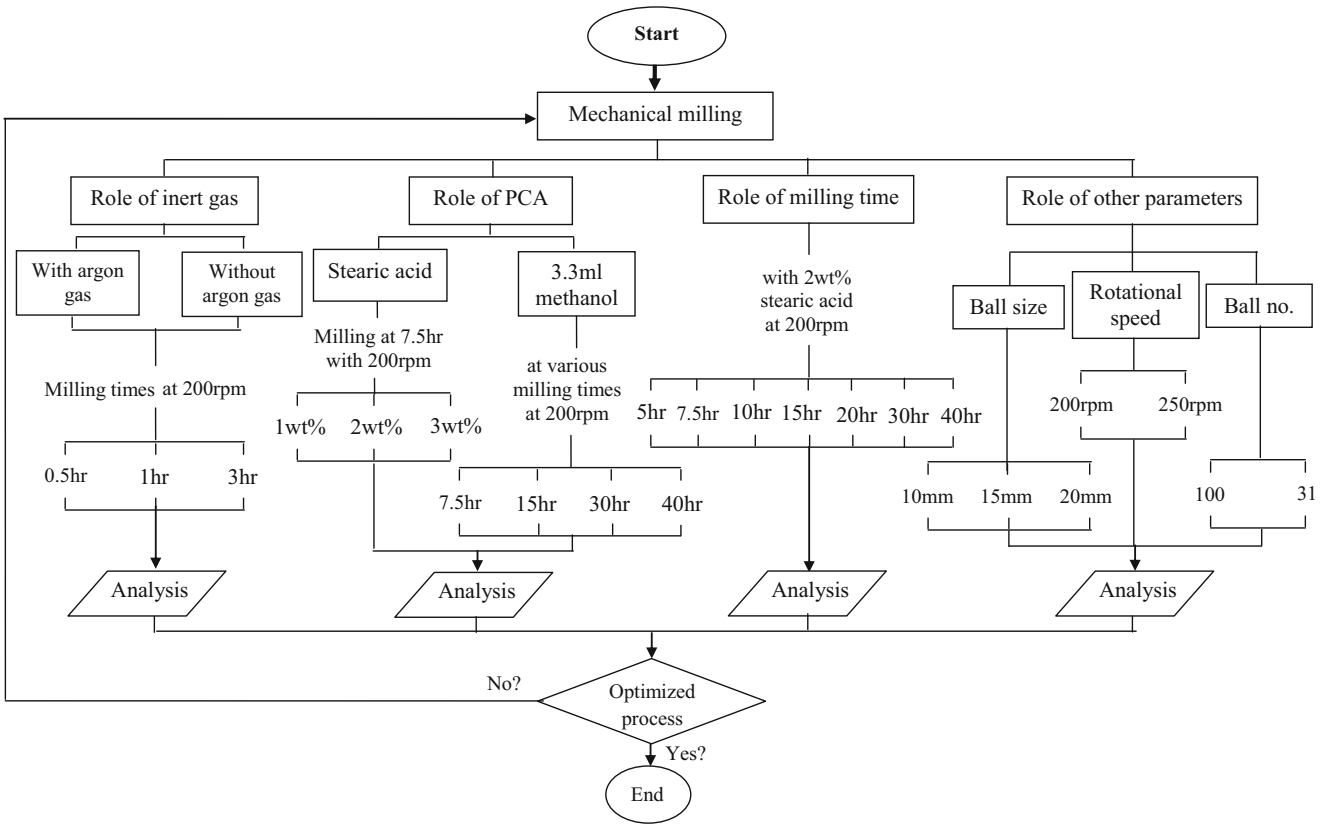

Fig. 2 Methodological framework of the mechanical milling

Table 1 Summary of milling parameters

Al	Ball no.	Ball size (mm)	Stearic acid (wt%)	Methanol (mL)	Speed (rpm)	Ratio (B/P)
0.5 h	100	10	–	–	200	10
1 h	100	10	–	–	200	10
3 h	100	10	–	–	200	10
5 h	100	10	2	–	200	10
7.5 h	100	10	–	–	200	10
7.5 h	100	10	1	–	200	10
7.5 h	100	10	2	–	200	10
7.5 h	100	10	3	–	200	10
7.5 h	100	10	–	3.3	200	10
10 h	100	10	2	–	200	10
15 h	100	10	2	–	200	10
15 h	100	10	2	–	250	10
15 h	31	15, 20	2	–	200	10
15 h	31	15, 20	2	–	250	10
15 h	100	10	–	3.3	200	10
20 h	100	10	2	–	200	10
30 h	100	10	2	–	200	10
30 h	100	10	2	–	250	10
30 h	31	15, 20	2	–	200	10
30 h	31	15, 20	2	–	250	10
30 h	100	10	–	3.3	200	10
40 h	100	10	2	–	200	10
40 h	100	10	2	–	250	10
40 h	31	15, 20	2	–	200	10
40 h	31	15, 20	2	–	250	10
40 h	100	10	–	3.3	200	10

motion to bring them in colliding positions. The amount of energy produced by the impact during milling is expected to be the source of crack propagation and fracture leading to the breakage of the work materials into smaller sizes.

Another consideration that should also be taken into account is the ratio of the amount of milling balls and work materials which is also known as B/P ratio (ball to powder ratio). This ratio is to ensure that the maximum amount of work material is in the collision with the maximum amount of milling balls. It has been emphasized that the most practicable B/P ratio is 10:1 (ten unit mass of ball against one unit mass of work materials).

2.1 Experimental materials

In this study, aluminum powder used was from Khorasan powder metallurgy, Iran, with a purity of >99 %. The particle size was 31.97 μm in diameter (90 %) and was in flake shape. A 40-g aluminum was ball-milled using a 500-mL stainless steel mixing jar (with 110 mm in inner diameter and height) of planetary ball mill of Retsch 400M with an effective sun wheel diameter of 300 mm and speed ratio of 1:−2.5, as shown in Fig. 1. During the process, the aluminum powder was milled at various milling times with 1 min pause followed by the change in turning direction after every 15 min. The jars were agitated with two different ball numbers of 31 and 100 up to 40 h, thus giving a ball to powder weight ratio (B/P) 10:1 to reach a fine powder particle size regarding to powder morphology.

Milling parameters have been varied accordingly in order to attain the optimum milling conditions for aluminum matrix as shown in Fig. 2. Initially, the aluminum was milled at three different milling times of 0.5, 1, and 3 h at 200 rpm. Mixing was carefully controlled under inert gas in order to avoid impurities. Impurities in sample will influence the physical, interface reaction, and mechanical properties of milled aluminum. In addition, similar millings were also performed

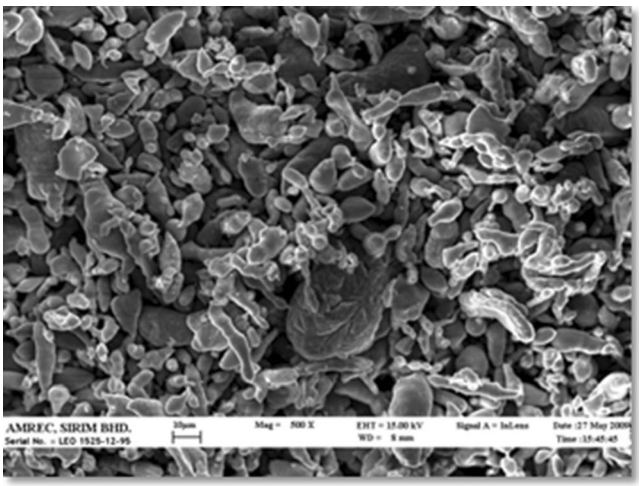

(a)

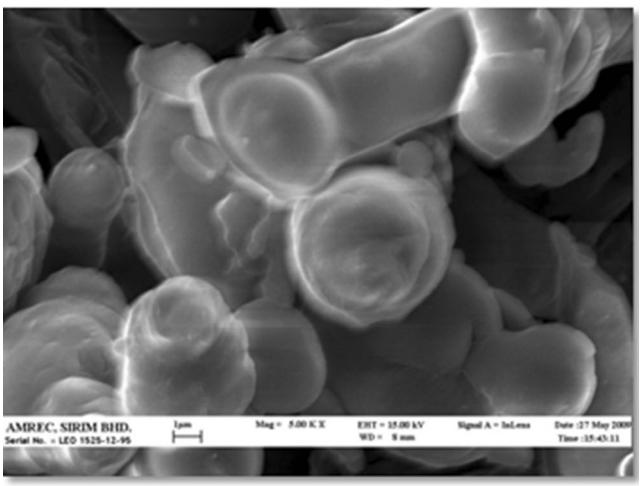

(b)

Fig. 3 **a** SEM and **b** FESEM micrographs of the pure (unmilled) aluminum powder

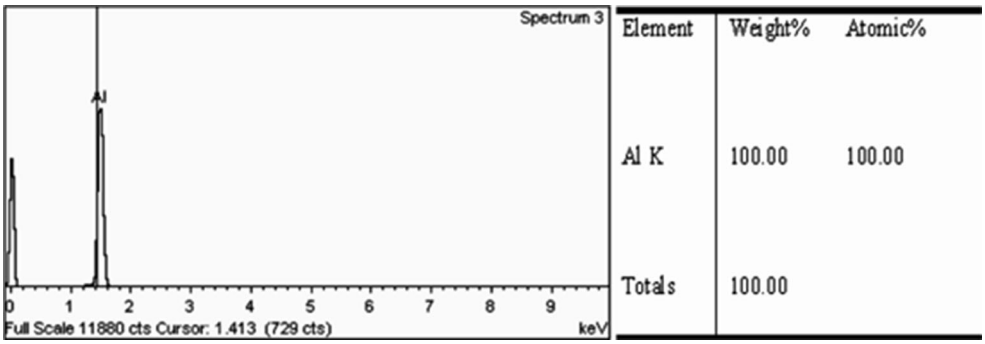

Fig. 4 EDX analysis of pure aluminum

without the argon gas to verify the effect of the inert gas on the quality of the particles.

Then, the effect of process control agent (PCA) was investigated with 1–3 wt% stearic acid [$CH_3(CH_2)_{16}COOH$] added during 7.5 h of milling to minimize the cold welding of the aluminum particles. In addition, the PCA was used to prevent powders from sticking to the balls and the jar wall. The investigation was continued with the milling of aluminum powder at seven various milling times from 5 to 40 h (5, 7.5, 10, 15, 20, 30, and 40 h) with 2 wt% stearic acid. The rotational speed remained at 200 rpm throughout this investigation.

For further study on the mechanical milling parameters, stainless steel ball size was changed from 10 mm (100 balls) to 15 and 20 mm (different balls, DB), but keeping the same B/P ratio of 10:1. Subsequently, the rotating speed has also been changed from 200 to 250 rpm (different speeds, DS), and finally, both ball size and rotational speed were changed (DB-DS) with inclusion of 2 wt% stearic acid of PCA. The milling was then carried out to 40 h (7.5, 15, 30, and 40 h) with 200 rpm speed, 100 balls (10 mm in diameter), but with 3.3 mL methanol in order to examine the effect of different PCAs on the morphology, particle size, and contamination of the aluminum matrix. The milling parameters are summarized accordingly in Table 1.

2.2 Experimental analysis

The particle size and distributions of powders were determined using a particle analyzer of CILAS 1190 instrument with a measurement range from 0.04 to 2,500 μm to examine the effect of various milling parameters. An energy dispersive

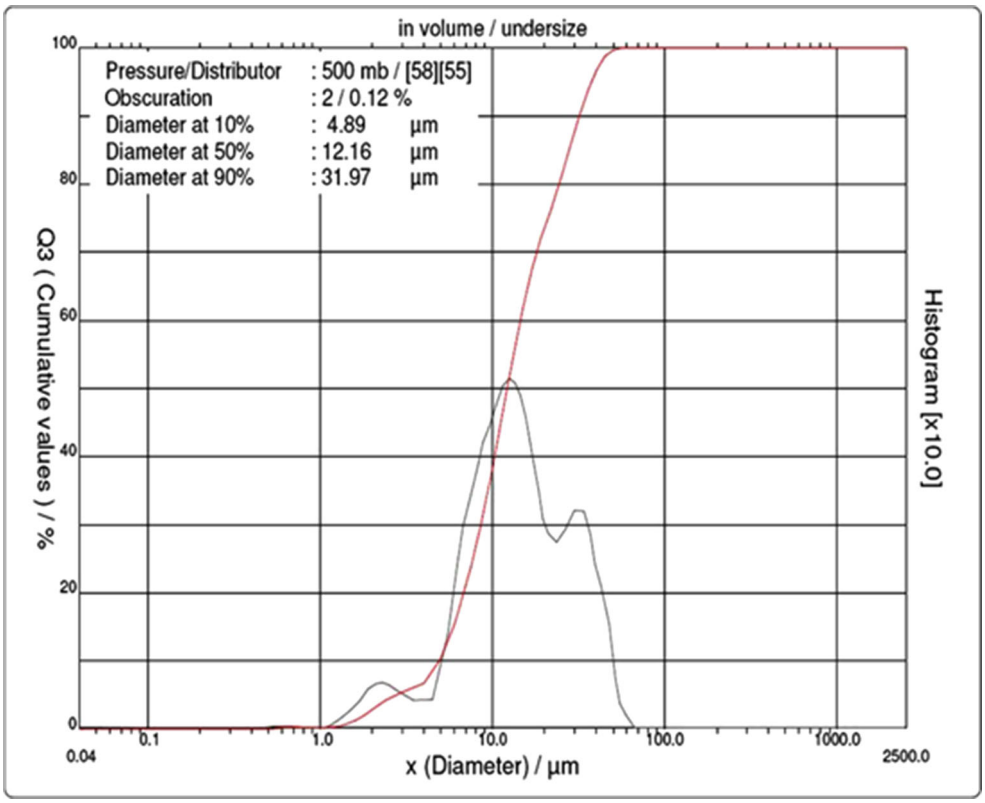

Fig. 5 Particle analyzer graph (CILAS 11900) of pure aluminum

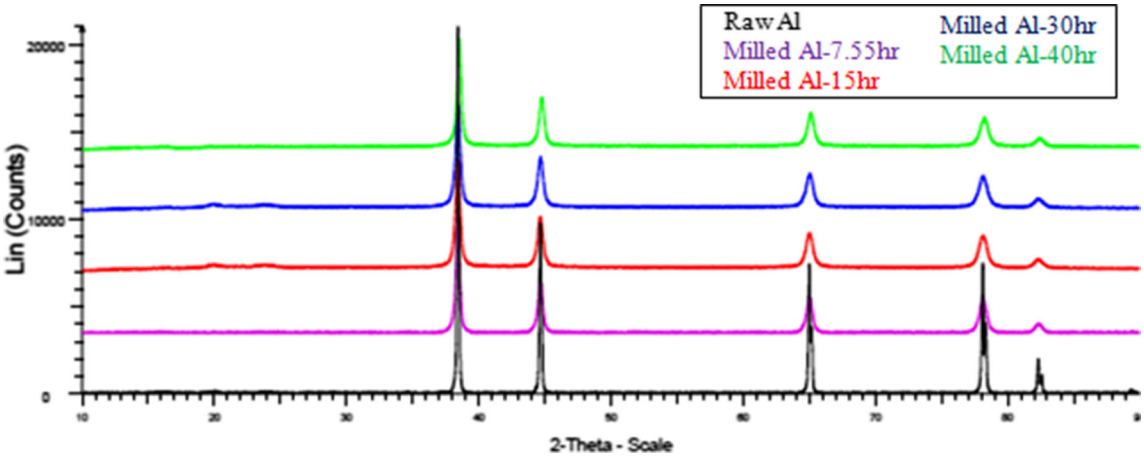

Fig. 6 X-ray diffraction (XRD) pattern of pure (unmilled) and milled aluminum powder

X-ray (EDX) analysis using a field emission scanning electron microscope (FESEM) model LEO supra 55 with up to 40 nA probe current was also used to observe the powder morphology and contamination of the powder.

On the other hand, an X-ray diffraction (XRD) characterization of the powders was performed with a Bruker type using $C_u K_\alpha$ radiation at 4.8 kW to define the essential quality and crystallography of the existing elements in aluminum. Thermal and oxidation stability of materials and phase transformation during mechanical milling process were also studied with thermo gravimetric analyzer (TA instruments SDTQ600) to specify any possible change in melting point of the powder after each setup of milling parameters.

3 Results and discussion

3.1 Powder morphology characterization

The raw material characterizations involved the determination of size, particle distribution, and morphology of aluminum powder were characterized by scanning electron microscope (SEM), EDX, laser particle measurement, XRD analysis, and differential scanning calorimeter (DSC). The aluminum powder morphologies in low and high magnification are shown in Fig. 3, while Fig. 4 exhibits the purity of aluminum powder with the EDX analysis. It was found that aluminum powder comprised of an average particle size of 31.97 μm as shown by the particle analyzer graph in Fig. 5. Due to a

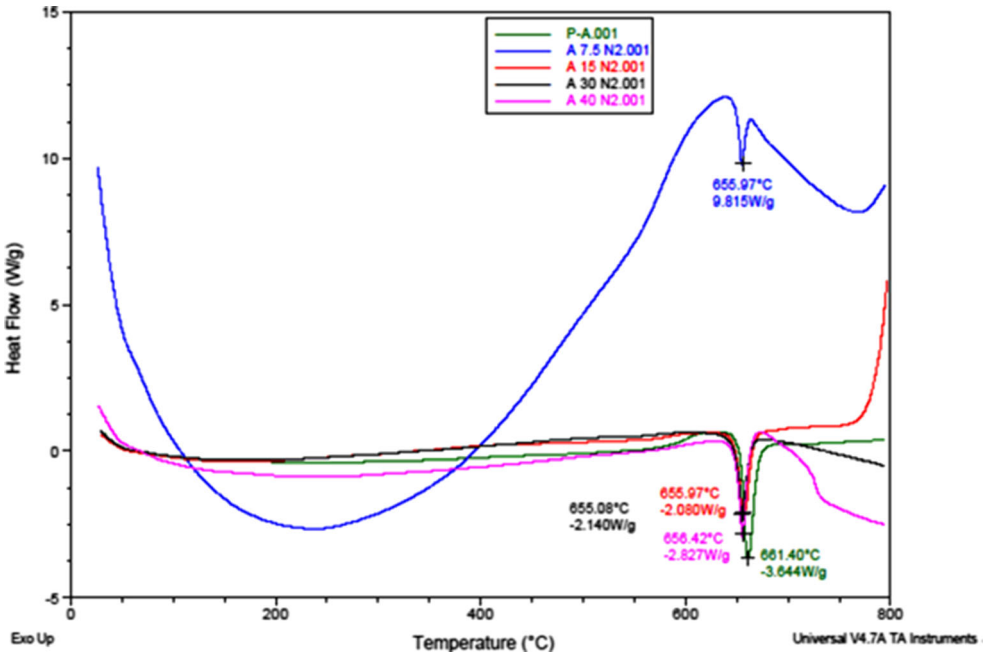

Fig. 7 DSC graph of pure (unmilled) and 15–30 h milled aluminum powder

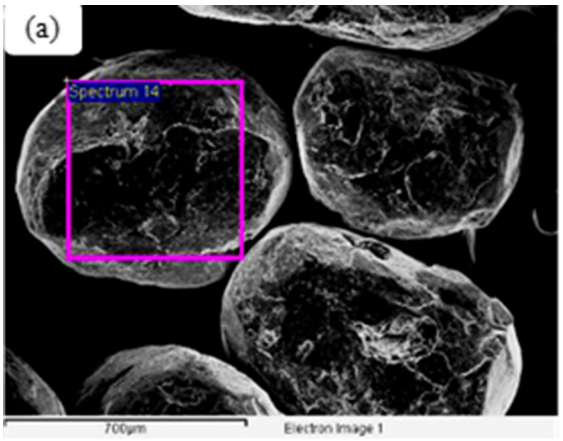

Element	Weight%	Atomic%
C K	5.36	11.12
O K	2.40	3.73
Al K	92.24	85.15
Fe K	0.00	0.00
Totals	100.00	

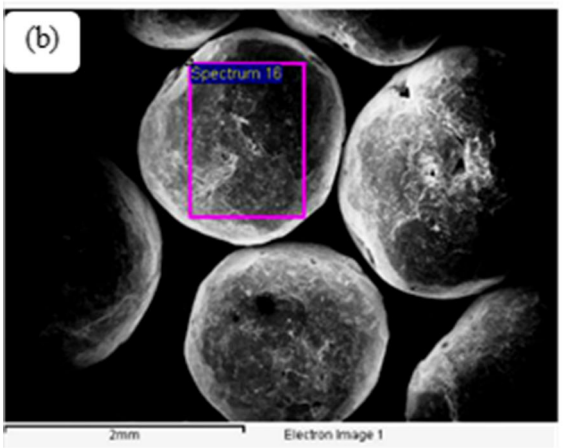

Element	Weight%	Atomic%
C K	5.16	10.64
O K	3.58	5.54
Al K	91.27	83.82
Fe K	0.00	0.00
Totals	100.00	

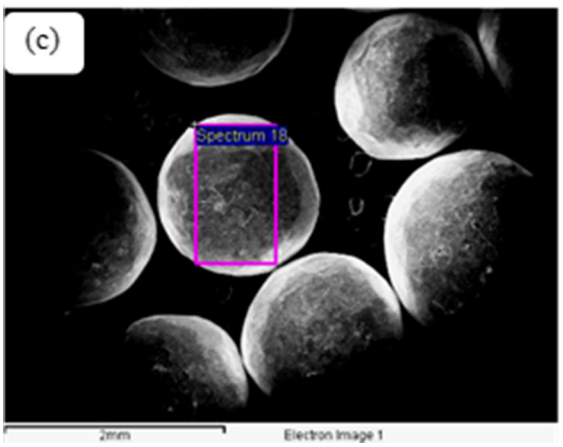

Element	Weight%	Atomic%
C K	6.88	13.95
O K	3.22	4.90
Al K	89.90	81.15
Fe K	0.00	0.00
Totals	100.00	

Fig. 8 SEM micrographs and EDX analysis for **a** 0.5 h; **b** 1 h; and **c** 3 h milled aluminum with argon

wide range of particle size, milling was required to attain a homogenous particle size distribution.

In addition, Fig. 6 illustrates the XRD analysis of the milled aluminum powders for 7.5, 15, 30, and 40 h that were carried out throughout this study. Five peaks were observed at $2\theta =$ 38.5°, 44.9°, 55.0°, 78.0°, and 82.5°. The observed lattice peaks of aluminum were very close to the reference value of 0.40 nm, suggesting the good quality and distribution of crystallites in the samples. In addition, the results provided indication of the amount of aluminum purity in the samples. In comparison to the pattern of starting (unmilled) powders, the milled counterparts showed a broadened intensity which indicated that the powder size was effectively reduced after milling.

DSC analysis has further proved the existent of pure aluminum powder (9.171 mg) using Pt pan at 10 °C/min temperature rate for 2 h and 40 min as shown in Fig. 7. The melting points of unmilled as well as 7.5–40 h milled aluminum were almost the same (~660 °C), which suggested that the milling process did not cause a major effect on the output of the DSC

analysis and could be useful for controlling milling temperature to avoid any phase changing or carbide formation during powder preparation.

3.2 Effect of the milling parameters in mechanical alloying of aluminum matrix

In this work, the milling parameters were varied to attain an optimized aluminum matrix particles size and ameliorative aluminum particle morphology. Reaching to smaller particle size with fine distribution is one of the challenges in milling of aluminum. On the other hand, a shift in particle morphology from flake to spherical with minimum particle size was achieved through this study. By having a spherical shape with smallest possible particle size would be advantageous in the preparation of metal matrix composites and sintering processes.

3.2.1 Role of inert gas in MA

The aluminum particles were milled for 0.5, 1, and 3 h with 100 balls (10 mm in diameter) at 200 rpm rotating speed, without PCA. Argon gas was applied to aluminum powder during the milling process. The SEM micrographs shown in Fig. 8 indicated a shifting of the morphology of particles from flake to spherical shape and an increase in particle size, through welding and agglomeration with a rough surface up to ~1.5 mm after 1 h milling. The exception was observed after 3 h of milling which the particle size was reduced due to higher impact force and temperature increase inside the jar that induced particles toward higher density and lower porosity form as well as closer to spherical shape. Although spherical shape is more suitable for diffusion during sintering and compaction process but it is not without limitation. In beside, smaller particle sizes which act as matrix in combination with reinforcements for producing nano-composites are advisable.

The level of contamination was also monitored by EDX analysis as shown in Fig. 8, which indicated a low contamination level for all of those milling condition (0.5–3 h milling). In addition, Fig. 9 highlights the changes in aluminum particle size for 0.5–3 h of milling time without argon gas. It was noticed that without the argon gas, the aluminum particles were found melted and trapped to the jar wall after 30 min of milling. Thus, for further experimental work on the optimization of milling parameters, argon gas was applied in all the milling processes.

3.2.2 Role of milling time in MA

In this study, 2 wt% of stearic acid (as a PCA) was added to the aluminum matrix powder with the milling performed at 200 rpm rotational speed with 100 balls (10 mm in diameter). Subsequently, the milling times were increased from 5 up to

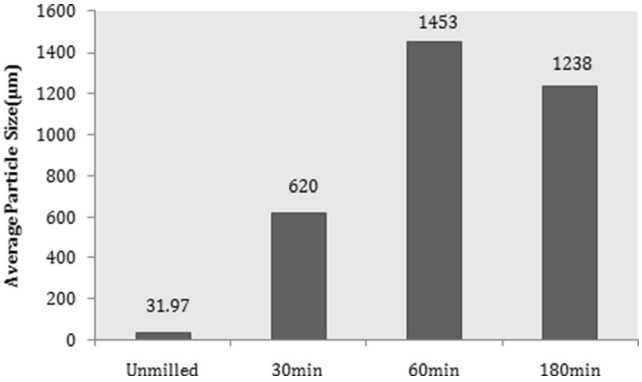

Fig. 9 Laser particle analysis for pure (unmilled) and 0.5–3 h milled aluminum without argon and PCA

40 h (5, 7.5, 10, 15, 20, 30, and 40 h, accordingly) to examine the effect of milling time on aluminum powder shape, size, and contamination level.

Figure 10 shows series of SEM micrographs of 5–40 h milled aluminum powders together with those of the unmilled pure aluminum for an immediate comparison. In addition, Fig. 11 highlights the results of average particle sizes obtained using the laser particle analyzer of pure and milled aluminum at different milling times. It was found that the aluminum matrix produced different plots when the milling times were changed. The main particle size was increased from 31.97 to 89.93 μm after 5 h of milling due to welding mechanism, and agglomerate of the aluminum powder was found higher than fracturing. It was then decreased until 69.81 μm (15 h of milling) as a result of the ball impact and friction, and again was increased continuously up to 216.175 μm for 40 h of milling.

The latter was attributed to rapid increase in temperature during the milling process, in which after a certain temperature, the PCA was unable to control the cold welding from occurring. At this stage, warm welding has occurred instead, depending on the powder melting point. Even at this stage, the impact energy was insufficient enough to break down the particle (sometimes the temperature and pressure could reach to 500 °C and 500 KPa, respectively). Generally, the particle size and shape were very important factors in the preparation of aluminum matrix, although contamination (O, Fe, and C) and phase change were investigated by EDX as well.

3.2.3 Role of PCA in MA

At the 7.5 h of milling with 100 balls (10 mm in diameter) and 200 rpm speed, 1–3 % of the stearic acid was added. Figures 12 and 13 show the results from the morphology analysis; it was shown that the aluminum particles started to weld together and formed large particles with a rough surface. It has been observed that some particles have approached 490.16 μm in size (which then impact energy of the balls contributed to the flakes shape) and a particle size of ~90 μm

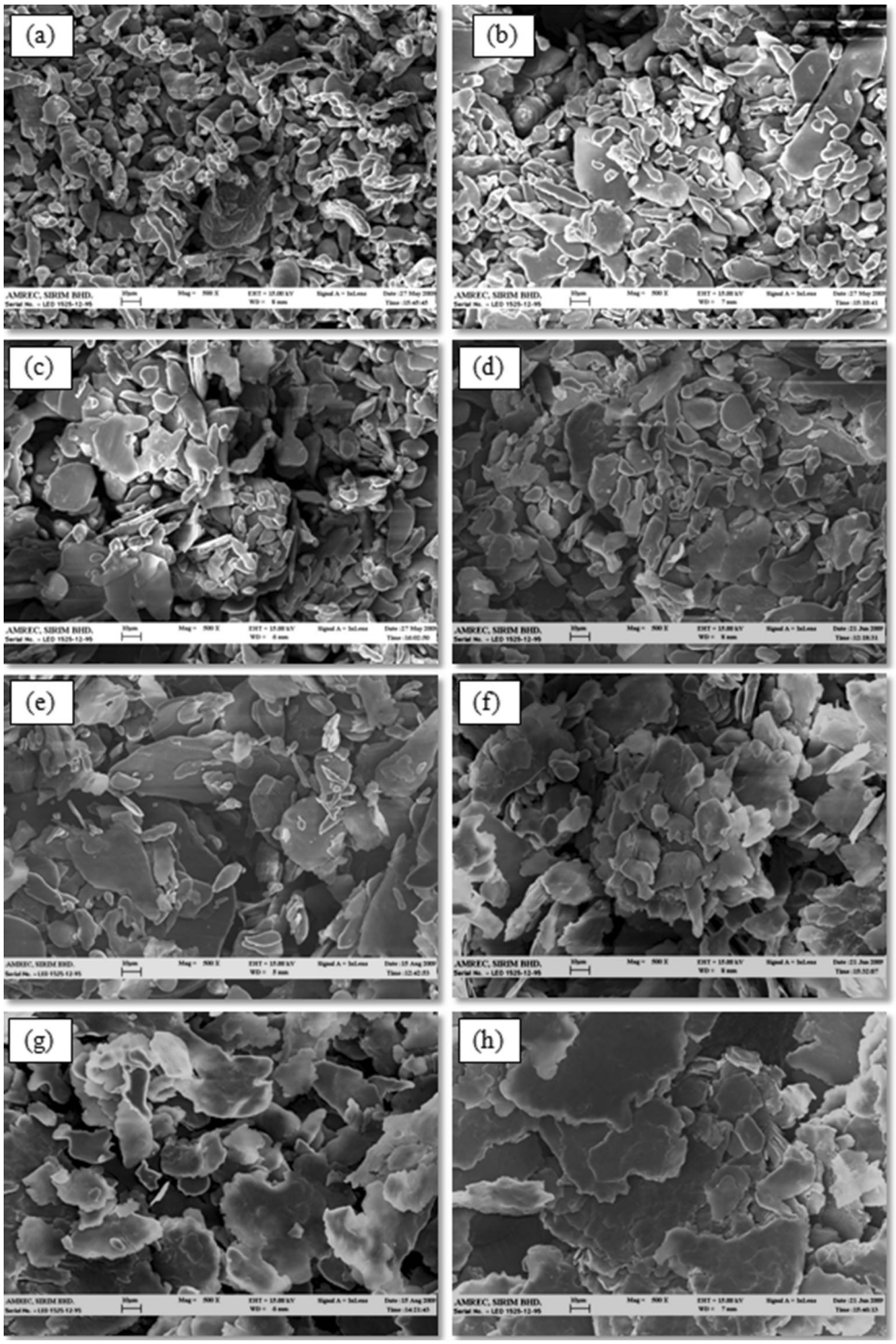

Fig. 10 SEM micrographs for **a** raw (unmilled); **b** 5 h; **c** 7.5 h; **d** 10 h; **e** 15 h; **f** 20 h; **g** 30 h; and **h** 40 h milled aluminum powder

when milling was continued under the stearic acid. In fact, without adding any amount of PCA, a more spherical shape or a conversion from the flake shape of original powder to spherical could be obtained, which has better feature for sintering process rather than a flake shape, but reaching to smaller particle size becomes challenging. The option would be either (i) to prepare the aluminum in both bigger particle size and closer to spherical shape, or (ii) to prepare fine particles but flake in shape, as metal matrix in composite with higher diffusion rate in powder consolidation applications.

It has been observed that without the PCA, the particle size of aluminum powder has increased substantially from 31.97 μm of unmilled powder to 490.16 μm after 7.5 h of milling time. As shown in Figs. 12 and 13, the PCA (stearic

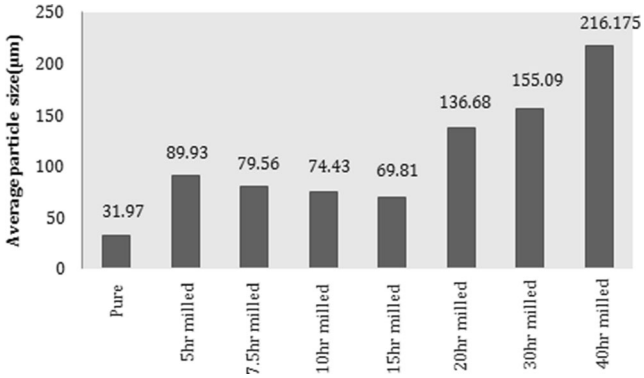

Fig. 11 Laser particle analysis of pure (unmilled) and milled aluminum in different milling times

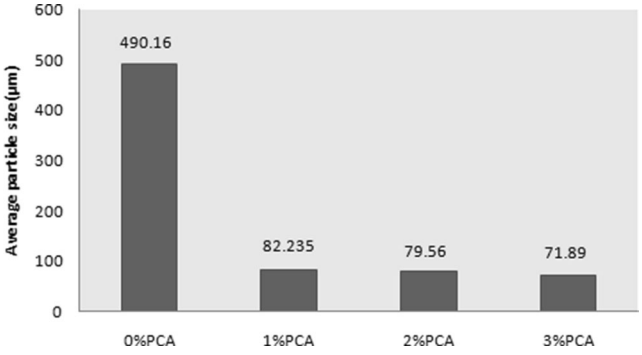

Fig. 13 Laser particle analysis of 7.5 h milled aluminum in 0–3 wt% of stearic acid

acid) was added to overcome fracture mechanism to cold welding. After subsequently adding up to 3 wt% of PCA, the particle size has reached to 71.89 μm and morphology was changed from flake to more equiaxed shape with lower yield. It was anticipated that in order to effectively control the effects of agglomeration and inhomogeneous particle size was through the changing of the PCA to methanol. The alternative PCA could provide a mechanism to prevent the cold welding of the particles and hence, the agglomeration to occur, resulted in the alteration of the morphologies.

As the milling was carried out with the new PCA (i.e., 3.3 mL methanol), it was evidently shown in Figs. 14 and 15 that the sizes of aluminum powder have reduced to 8.93 μm after 30 h of milling from 31.97 μm for pure aluminum. It was believed that the methanol has a more effective technique to create the breaking mechanism compare to the cold welding. However, the particles started to agglomerate, causing an increase in the size from 8.93 to 11.85 μm as the milling time was increased to 40 h. This could be attributed to the low melting temperature of aluminum, in which the heat inside the milling jar intensified and agglomeration occurred causing the particle size to increase accordingly as the milling progressed.

3.2.4 Role of ball size, ball number, and rotation speed in MA

In this section, the size of milling ball was increased to 15 and 20 mm, but the quantity was reduced to provide the same B/P ratio of 10:1. By using the total number of 31 balls with 15 and

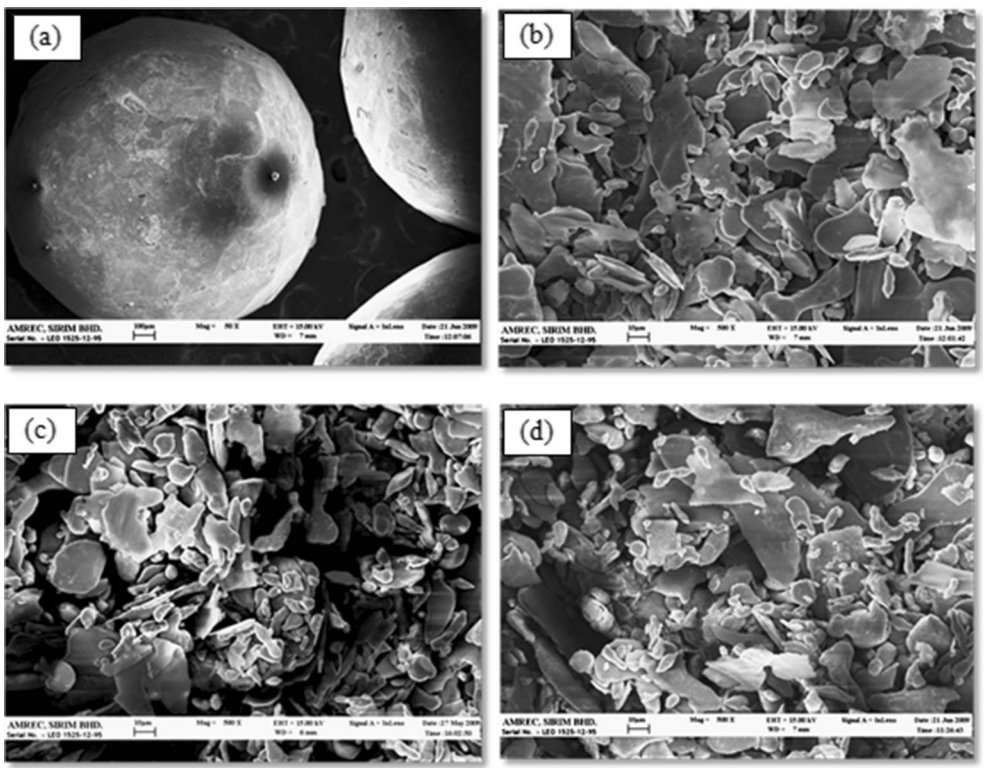

Fig. 12 SEM micrographs of 7.5 h milled aluminum with **a** 0 wt%; **b** 1 wt%; **c** 2 wt%; and **d** 3 wt% of stearic acid

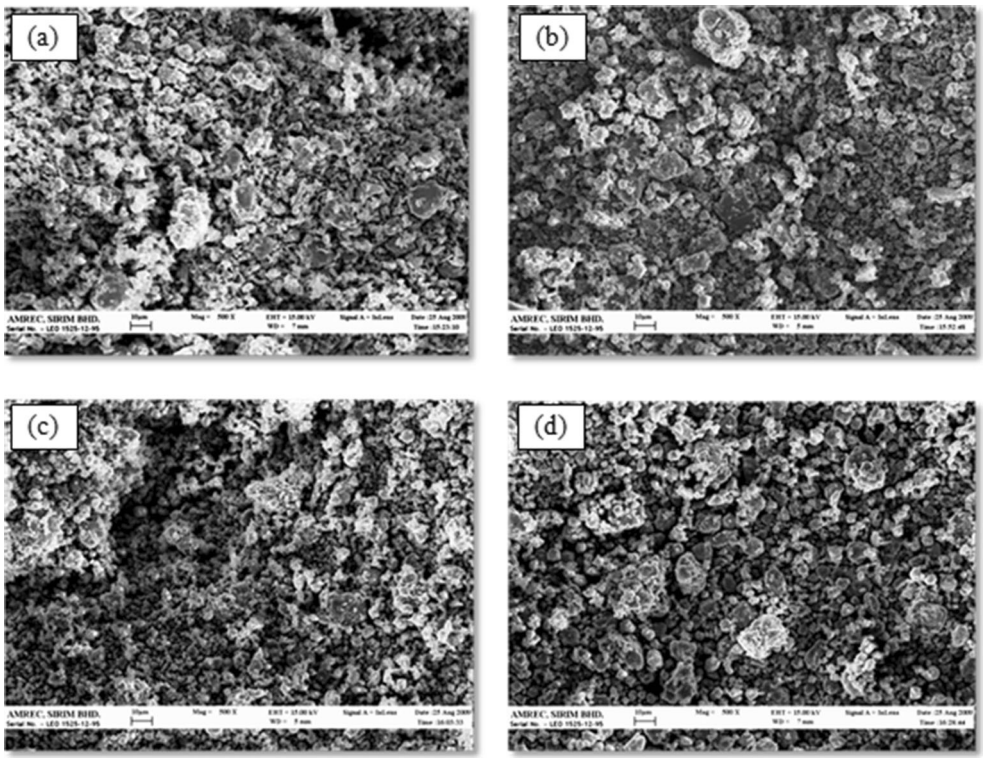

Fig. 14 SEM micrographs of **a** 7.5 h; **b** 15 h; **c** 30 h; and **d** 40 h milled aluminum with methanol

20 mm ball size and 250 rpm rotational speed, the ball impact energy has been accrued and, at the same time, the temperature inside the jar has also been increased as well.

Figure 16 provides the results of SEM micrograph for six different conditions. The sequence of (a) to (c) indicated the change in the particle size and arrangement of the milled aluminum at 15 h milling time with different ball numbers and sizes, as well as rotating speed. As a result, after 15 h of milling, particle size and distribution have dramatically changed as different ball numbers and sizes were used. As the ball size was increased, the colliding impact per ball has intensified, but the overall milling rate may well reduce due to the increased weight and inertia. This has caused higher occurrence of welding and agglomeration of the aluminum powder than the fracturing mechanisms as the impact energy increased.

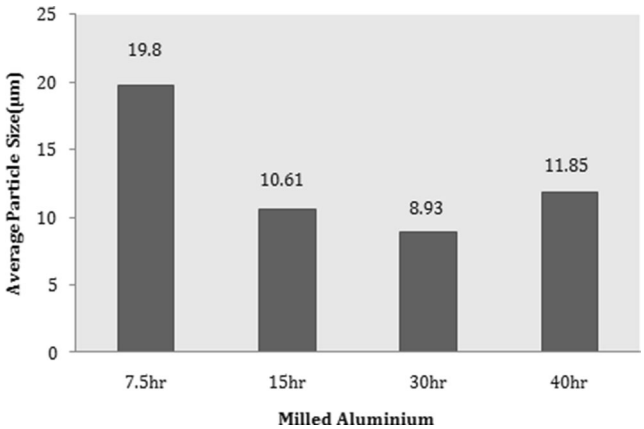

Fig. 15 Laser particle analysis for 7.5–40 h milled aluminum with methanol

The particle morphologies were further altered when the rotating speed was increased to 250 rpm. Higher colliding speed has promoted the aluminum particles to weld together and form larger particles, contributing to the flakes shape. In addition, the average particle sizes were obtained using the particle analyzer, in which the changes for the first three conditions (i.e., milled at 15 h) were clearly summarized in Fig. 17. It has been observed that the average size was increased from 31.97 to 85.81 μm when the ball number and size were changed, and then further increased considerably to 221.35 μm with higher rotation. The changes in the particular milling parameters have considerably increased the collision intensity between the milling balls and aluminum powders, hence the welding formation, contributing to the higher particle sizes.

This trend has continued for those aluminum particles milled at 30 h. The sequences of Fig. 16d–f have indicated that with the changes in milling parameters (i.e., milling balls and rotating speed), the morphologies of the aluminum particles have changed to agglomerated particle in which the average particle size has reached up to 259.89 μm, as summarized in Fig. 18. However, when the milling time was further increased to 40 h, then only the average particle size has slightly decreased from 216.17 to 199.24 μm, as shown in Fig. 19; this was due to double break and fracture of half melted particle, which attributed to very high impact energy.

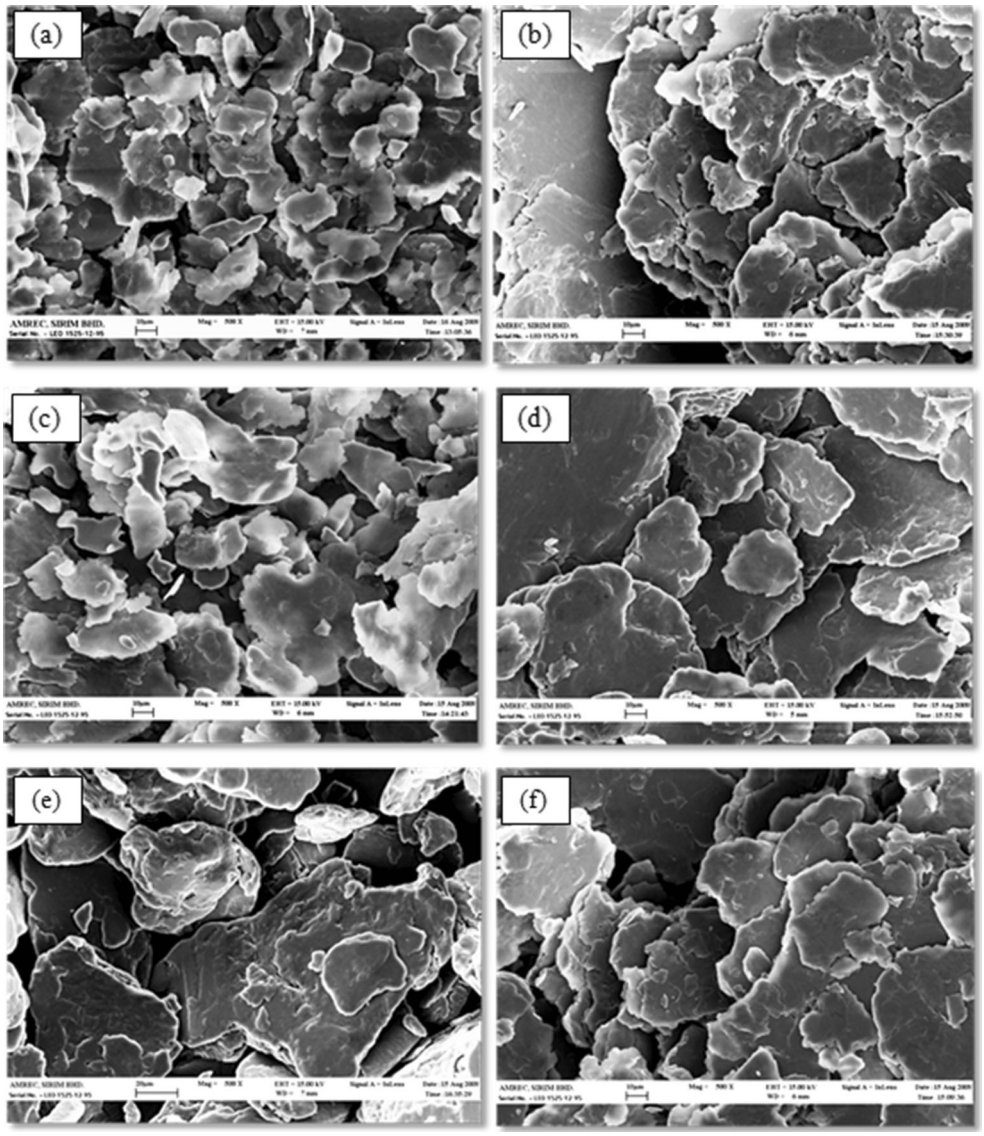

Fig. 16 SEM micrograph for **a** 15-h milled aluminum; **b** 15-h milled aluminum, DB; **c** 15-h milled aluminum, DB-DS; **d** 30-h milled aluminum; **e** 30-h milled aluminum, DB; **f** 30-h milled aluminum, DB-DS. [*DB*, different ball number and size: 31 (10–15 and 20 mm) balls; *DS*, different rotation speed (250 rpm)]

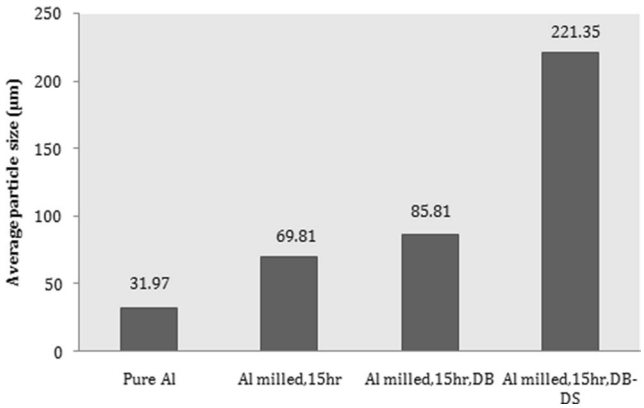

Fig. 17 Laser particle analysis of 15-h milled aluminum in different ball size (10, 15, 20 mm), ball no. (31), and rotation speed (250 rpm) in comparison with the pure (unmilled) aluminum

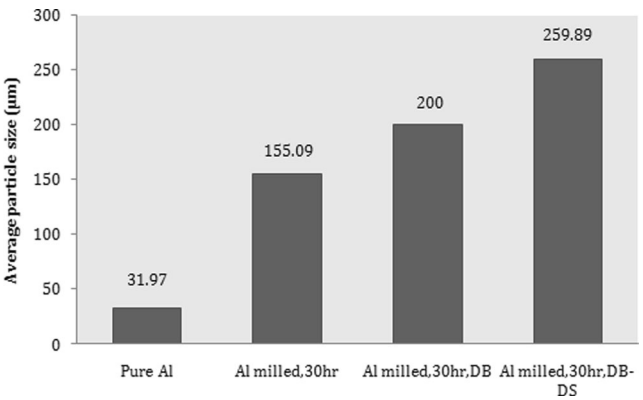

Fig. 18 Laser particle analysis of 30-h milled aluminum in different ball size (10, 15 and 20 mm), ball no. (31) and rotation speed (250 rpm) in comparison with the pure (unmilled) aluminum

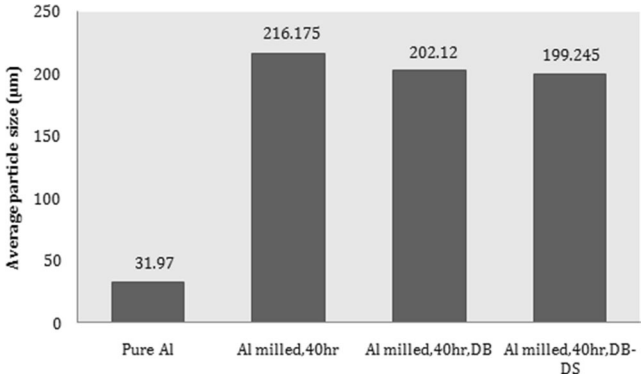

Fig. 19 Laser particle analysis of 40-h milled aluminum in different ball size (10, 15, and 20 mm), ball no. (31), and rotation speed (250 rpm) in comparison with the pure (unmilled) aluminum

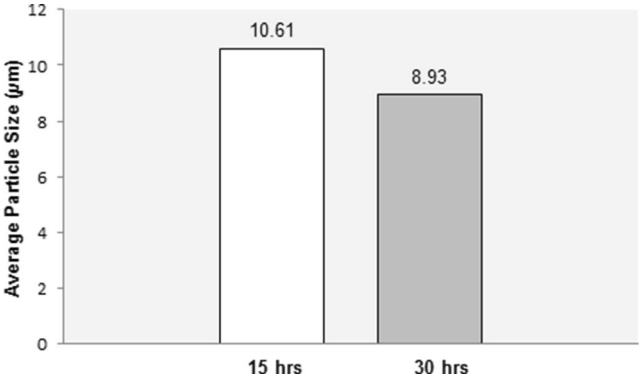

Fig. 21 Average particle sizes obtained using a laser particle analyzer for 15-h- and 30-h milled aluminum matrix, accordingly

In this stage, the contamination level (Fe and O) was high with EDX scans of the specimens and powder morphology was inhomogeneous with the mixing of flake and agglomerated particles.

It was anticipated that with the average powder sizes obtained for the aluminum of above 250 μm can be so large, that it could prevent any possibility of sintering to occur in the upcoming process. As indicated successfully in the previous section, one possible way to control this effect (i.e., agglomerated and inhomogeneous particle distribution) is either through the changing of a PCA to methanol or by decreasing the impact energy from the ball collision onto the particles. The methanol has provided an effective mechanism to break the particle and prevented the agglomeration to occur, as well as altering the morphologies from flake-like shape to granular structures. With the reduced size and homogeneity of the particle distribution, it enables the powder to be used effectively during the sintering process of the aluminum matrix as a metal matrix to further produce optimized compacting bulk carbon nano-composites.

3.3 Experimental validation of the optimal milling parameters

Subsequently, the optimal milling parameters have been validated, where the coupling effects of different milling conditions on the morphology and structural evolution of mechanically alloyed aluminum powder were examined. The milling has included 100 stainless steel balls (10 mm in diameter), 200 rpm rotating speed with direction reversal, and 1 min pause time after each 15 min running time, with the process performed under the argon gas for 15 and 30 h, and 3.3 mL methanol was added as the PCA. Figure 20 shows the SEM micrographs of the milled aluminum powder after 15 and 30 h of milling. As the results of implementing those conditions, a shifting of the morphology of particles from flake to the spherical shape, with the formation of finer particle size, was observed. The adding of methanol as the PCA has helped in reducing the welding of the matrix particles that leads to the decrease in the particle size. The particular type of PCA provided the effective fracture mechanisms, which has modified the surface properties of the deforming particles to overcome the cold welding phenomenon.

In addition, further analysis on the average particle sizes have been carried out using the laser particle analyzer for 15 and 30 h of milling, as shown in Fig. 21. It was apparent that the latter condition has produced finer particle size, with the different of more than 15 % in the average size. With the methanol has successful prevented the agglomeration from occurring, a longer milling time would provide longer and repeated fracturing, effectively breaking the particles into

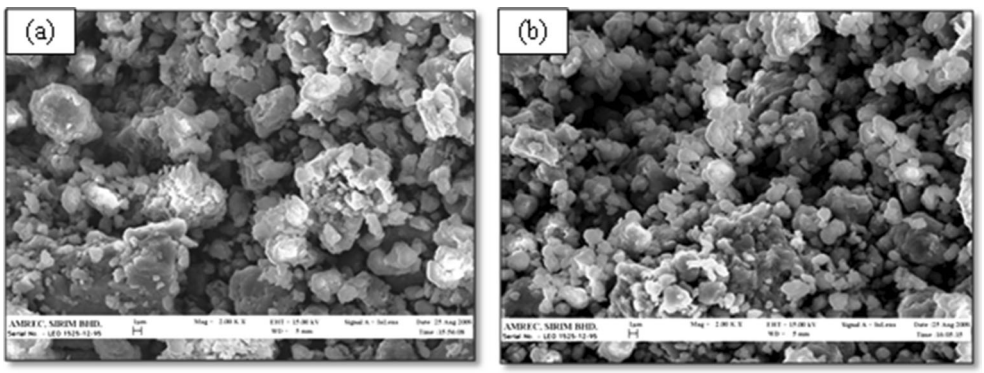

Fig. 20 SEM micrographs of **a** 15-h milled aluminum matrix; **b** 30-h milled aluminum matrix with optimal milling conditions

smaller size and changing the morphology from the flake to spherical shapes. This phenomenon was clearly contradictory than those mentioned earlier in Section 3.2.2, in which the longer milling times have caused larger size in the aluminum matrix. By having a spherical shape with smallest possible particle size, it would certainly be advantageous in the preparation of metal matrix composites through sintering process and subsequently could lead to better compaction quality.

4 Conclusion

The planetary mechanical alloying process of the aluminum powders has been observed, as the solid-state interfacial reaction of the particles was investigated upon inert gas, media ball number and size, milling time, speed, and PCA. The morphologies of the milled powder were found to significantly vary with different milling parameters, in which the formation of nanostructure and fine aluminum matrix particle size were observed in the study. In order to effectively prepare the aluminum powders as metal matrix for future sintering process and to produce further compacting carbon nano-composite, the milling parameters have been proposed to include 100 stainless steel ball (10 mm in diameter), 200 rpm rotation speed with direction reversal, and 1 min pause time after each 15 min running time, with the process performed under the argon gas for 30 h of milling. The use of methanol as the PCA has further reduced the particles size to 8.93 μm and underwent some changes in shape from flake-like structures to granular (disk) structures. However, the uses of different ball numbers and sizes, and with higher rotation speed have resulted in further agglomeration and poor homogeneity in particle distribution, thus preventing any possibility for the sintering of nano-composites.

Acknowledgments The authors would like to thank the Ministry of Higher Education, Malaysia, and Universiti Sains Malaysia for the financial support through the Fundamental Research Grant Scheme (FRGS) of 203/PMEKANIK/6071193 for this research work.

References

1. Benjamin JS (1992) Fundamentals of mechanical alloying. Mater Sci Forum 88–90:1–18
2. White RL (1979) The use of mechanical alloying in the manufacture of multifilamentary superconductor wire. Dissertation, Stanford University
3. Rairden JR, Habesch EM (1981) Low-pressure-plasma-deposited coatings formed from mechanically alloyed powders. Thin Solid Films 83:353–360
4. Schultz L (1988) Glass formation by mechanical alloying. J Less-Common Met 145:233–249
5. El-Eskandarany MS, Aoki K, Suzuki K (1992) Morphological and calorimetric studies on the amorphization process of rod-milled $Al_{50}Zr_{50}$ alloy powders. Metall Trans A 23:1992–2131
6. Novak BM (1993) Hybrid nanocomposite materials—between inorganic glasses and organic polymers. Adv Mater 5:422–433
7. He L, Ma E (1996) Full-density nanocrystallline Fe-29Al-2Cr intermetallic consolidated from mechanically milled powders. J Mater Res 11:72–80
8. El-Eskandarany MS, Omori M, Konno TJ, Sumiyama K, Hirai T, Suzuki K (1998) Syntheses of full-density nanocrystalline titanium nitride compacts by plasma-activated sintering of mechanically reacted powder. Metall Trans A 29:1973–1981
9. Nash P, Kim H, Choo H, Ardy H, Hwang SJ, Nash AS (1992) Metastable phases in the design of structural intermetallics. Mater Sci Forum 88–99:603–610
10. Hwang SJ, Nash P, Dollar M, Dymek D (1992) The production of intermetallics based on NiAl by mechanical alloying. Mater Sci Forum 88–99:611–618
11. Jain M, Christman T (1994) Synthesis, processing, and deformation of bulk nanophase Fe-28Al-2Cr intermetallic. Acta Metall Mater 42: 1901–1911
12. Oehring M, Appel F, Pfullmann T, Bormann R (1995) Mechanical properties of submicron-grained TiAl alloys prepared by mechanical alloying. Appl Phys Lett 66:941